



## PAPER

Monte Carlo dosimetric analyses on the use of  $^{90}\text{Y}$ -IsoPet intratumoral therapy in canine subjectsRECEIVED  
26 January 2024REVISED  
12 July 2024ACCEPTED FOR PUBLICATION  
25 July 2024PUBLISHED  
2 August 2024Mislav Bobić<sup>1,2,5</sup> , Carlos Huesa-Berral<sup>1,5</sup> , Jack F Terry<sup>1</sup>, Louis Kunz<sup>1,2</sup> , Jan Schuemann<sup>1</sup> , Darrell R Fisher<sup>3</sup>, Charles A Maitz<sup>4</sup>  and Alejandro Bertolet<sup>1,\*</sup> <sup>1</sup> Department of Radiation Oncology, Massachusetts General Hospital and Harvard Medical School, Boston, MA, United States of America<sup>2</sup> Department of Physics, ETH Zurich, Zurich, Switzerland<sup>3</sup> Versant Medical Physics and Radiation Safety, Richland, Washington, and University of Washington, Seattle, United States of America<sup>4</sup> Department of Veterinary Medicine and Surgery, University of Missouri, Columbia, MO, United States of America<sup>5</sup> These authors contributed equally to this work and share first authorship.

\* Author to whom any correspondence should be addressed.

E-mail: [abertoletreina@mgh.harvard.edu](mailto:abertoletreina@mgh.harvard.edu)**Keywords:** RadioGel, IsoPet, Y-90 therapy, soft tissue sarcomas, dog cancer models, dosimetry, comparative oncologySupplementary material for this article is available [online](#)**Abstract**

*Objective.* To investigate different dosimetric aspects of  $^{90}\text{Y}$ -IsoPet<sup>TM</sup> intratumoral therapy in canine soft tissue sarcomas, model the spatial spread of the gel post-injection, evaluate absorbed dose to clinical target volumes, and assess dose distributions and treatment efficacy. *Approach.* Six canine cases treated with  $^{90}\text{Y}$ -IsoPet<sup>TM</sup> for soft tissue sarcoma at the Veterinary Health Center, University of Missouri are analyzed in this retrospective study. The dogs received intratumoral IsoPet<sup>TM</sup> injections, following a grid pattern to achieve a near-uniform dose distribution in the clinical target volume. Two dosimetry methods were performed retrospectively using the Monte Carlo toolkit OpenTOPAS: imaging-based dosimetry obtained from post-injection PET/CT scans, and stylized phantom-based dosimetry modeled from the planned injection points to the gross tumor volume. For the latter, a Gaussian parameter with variable sigma was introduced to reflect the spatial spread of IsoPet<sup>TM</sup>. The two methods were compared using dose-volume histograms (DVHs) and dose homogeneity, allowing an approximation of the closest sigma for the spatial spread of the gel post-injection. In addition, we compared Monte Carlo-based dosimetry with voxel S-value (VSV)-based dosimetry to investigate the dosimetric differences. *Main results.* Imaging-based dosimetry showed differences between Monte Carlo and VSV calculations in tumor high-density areas with higher self-absorption. Stylized phantom-based dosimetry indicated a more homogeneous target dose with increasing sigma. The sigma approximation of the  $^{90}\text{Y}$ -IsoPet<sup>TM</sup> post-injection gel spread resulted in a median sigma of approximately 0.44 mm across all cases to reproduce the dose heterogeneity observed in Monte Carlo calculations. *Significance.* The results indicate that dose modeling based on planned injection points can serve as a first-order approximation for the delivered dose in  $^{90}\text{Y}$ -IsoPet<sup>TM</sup> therapy for canine soft tissue sarcomas. The dosimetry evaluation highlights the non-uniformity of absorbed doses despite the gel spread, emphasizing the importance of considering tumor dose heterogeneity in treatment evaluation. Our findings suggest that using Monte Carlo for dose calculation seems more suitable for this type of tumor where high-density areas might play an important role in dosimetry.

**1. Introduction**

Soft tissue sarcomas are tumors that arise from mesenchymal tissues, which means they can emerge from any anatomical site. In dogs, they most commonly occur in subcutaneous areas (Dennis *et al* 2010). As in humans, surgery is the primary treatment choice (Bray 2016, Hoefkens *et al* 2016). However, planning clear

margins is not always possible due to the invasive nature of the tumor. In fact, there are currently no diagnostic methods able to predict reliably the margins required. Adjuvant therapies like radiotherapy or chemotherapy have been used to maximize the benefit of surgical procedures (Bray 2016, Hoefkens *et al* 2016). Radiotherapy in combination with surgery has demonstrated shrinkage of resection margins without compromising patient outcomes (DeLaney *et al* 2005, Miller *et al* 2014). Aiming at improving the therapeutic index of radiotherapy, brachytherapy modalities have the potential to enhance the local dose to osteosarcoma tumors while limiting normal tissue exposures (Fisher *et al* 2020).

IsoPet™ therapy is a type of brachytherapy involving the intratumoral injection of <sup>90</sup>Y-phosphate (YPO<sub>4</sub>) mixed within a liquid polymer solution (room temperature) that solidifies (gels) at body temperature (Fisher *et al* 2020). It provides a constrained yttrium-90 (<sup>90</sup>Y) source for highly localized radiotherapy with minimal exposure to the surrounding healthy tissue. The mechanism of IsoPet™ is intended to concentrate radiation in the tumor in a direct and controlled way. <sup>90</sup>Y emits beta particles with a penetration range of 11 mm with an average range of 2.5 mm. While current standard of care radiation therapy for soft tissue sarcomas is typically performed using external beam radiotherapy (Withrow 2007, Bray 2016), the highly localized IsoPet™ therapy may improve normal tissue sparing and therefore reduce the risk of potential radiation-induced toxicities.

Dosimetry plays a crucial role in the safe and effective delivery of radiation therapy. The absorbed dose has been shown to strongly correlate with tumor control and toxicity induction in all cancer treatments involving the use of ionizing radiation (Bentzen *et al* 2010, Chansanti *et al* 2017, Garin *et al* 2020). In the case of IsoPet™, the distribution of <sup>90</sup>Y radionuclides can vary locally, potentially affecting how tumors respond to a given absorbed dose, i.e. the average energy imparted per unit mass in the tumor. A comprehensive dosimetric analysis can provide insights into this spatial distribution, dose deposition patterns, and potentially guide tailoring of clinical treatment plans, optimizing prescription, and administration.

While IsoPet™ has shown promise in animal studies regarding safety (Fisher *et al* 2018, Fisher 2021) and therapeutic response (Fisher *et al* 2020), dosimetric studies to analyze potential ways of optimization are still limited. Cantley and colleagues studied the application of IsoPet™ to ocular melanoma using Monte Carlo methods to elucidate whether <sup>90</sup>Y beta emissions may result in unacceptable doses in critical ocular structures, showing potentially toxicity-eliciting doses for large tumors located at posterior areas of the eye (Cantley *et al* 2017). However, this study considered uniform distributions of <sup>90</sup>Y in the melanoma volumes, disregarding how the polymer solution distributes after solidification. Fisher and colleagues provided PET-CT-based dosimetry as an initial insight for a canine trial conducted at the University of Missouri. Yet, deeper dosimetric analyses are encouraged (Fisher *et al* 2020).

The present study focuses on extended dosimetric considerations associated with <sup>90</sup>Y-IsoPet™ intratumoral therapy in six canine cases treated at the Veterinary Health Center at the University of Missouri. We apply Monte Carlo calculations and a dosimetric analysis to investigate the spatial distribution of the gel post-injection, validating the dose prescription procedures and comparing results to the available information from PET-CT scans acquired after treatment administration. This study aimed to lay the groundwork for optimizing treatment planning designs to enhance therapeutic outcomes for both pets and, eventually, translation to solid tumors in humans.

## 2. Materials and methods

### 2.1. Patient population

Six dogs with naturally occurring soft tissue sarcomas were prospectively enrolled in a pilot study at the University of Missouri Veterinary Health Center. The dogs were diagnosed with naturally occurring, cytologically or histologically confirmed soft tissue sarcoma that were accessible for intralesional <sup>90</sup>Y-IsoPet™ administration. Dogs of any age, breed, or sex were included, provided they weighed more than 5 kg, had gross disease, and the tumor was superficial and accessible to brachytherapy. Dogs with significant comorbidities that could complicate anesthesia or hospitalization (i.e. cardiac, renal, or hepatic insufficiency) were excluded, as well as dogs that had received chemotherapy within three weeks prior to treatment. Additional details for each individual dog are summarized in table 1.

### 2.2. Injection procedure and treatment planning

The injection procedure was described previously (Fisher *et al* 2020). First, the canine patients were anesthetized. The tumor surfaces were disinfected and marked with a regular and parallel two-dimensional (2D) grid pattern for all the intratumoral injections, facilitating the placement of IsoPet™ uniformly within the tumor. Intended, or prescribed doses, were aimed to be delivered uniformly to the tumors, and the positions of the needles were determined accordingly. Each injection was administered using a continuous flow as the needle was withdrawn from the farthest point within the tumor to a point directly opposite. The

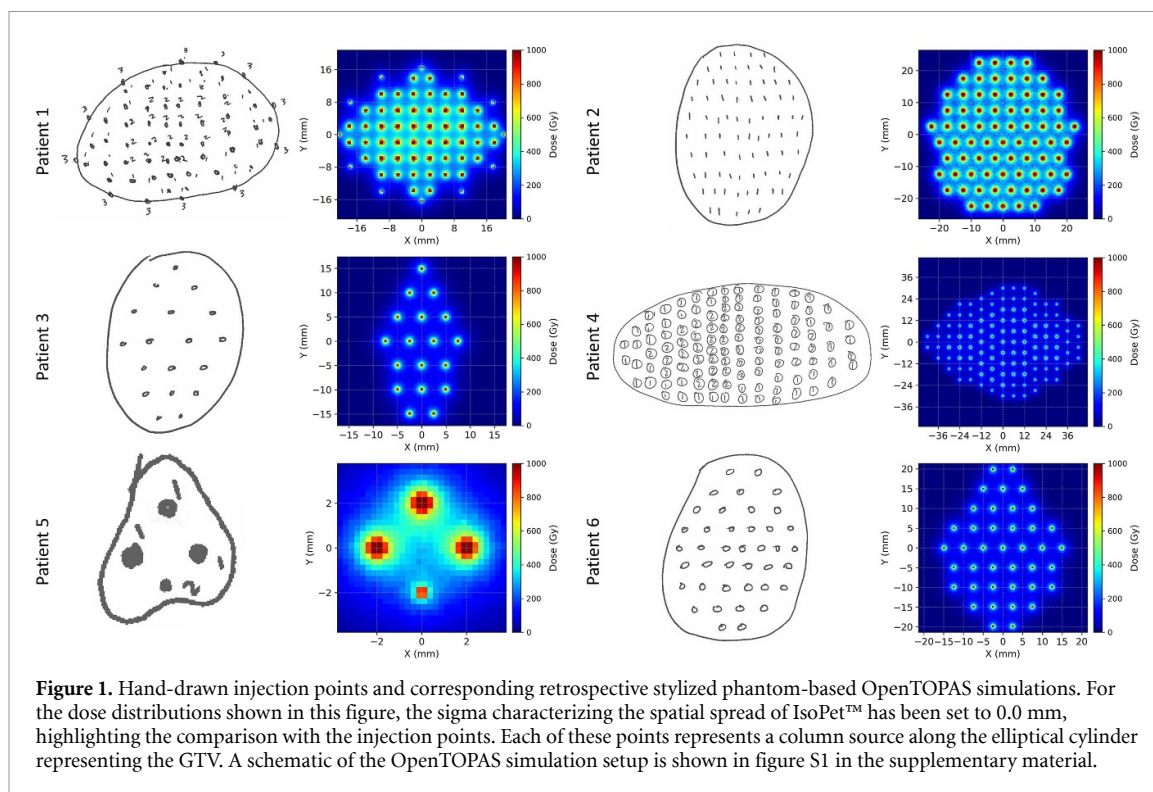
**Table 1.** Canine patient population.

Clinical Description and Outcome						
Canine patient	Signalment	Tumor dimensions	Activity planned (MBq)	Prescribed mean tumor dose (Gy)	Maximal response	Final status
Patient 1	10 year-old male Shetland sheepdog; Soft tissue sarcoma of the caudal right thigh	$5.1 \times 5.6 \times 4.0 \text{ cm}^3$ 60.6 ml GTV	435.06	300	Complete response	Progressive disease
Patient 2	11 year-old male Shetland sheepdog; Soft tissue sarcoma of the caudal right thigh	$5.1 \times 5.6 \times 4.0 \text{ cm}^3$ 95.0 ml GTV	710.25	255	N/A	N/A
Patient 3	10 year-old spayed female Labrador mix; Soft tissue sarcoma on the medial aspect of the right pelvic limb	$60 \times 32 \times 28 \text{ cm}^3$ 55.4 ml GTV	170.46	300	Progressive disease	Progressive disease
Patient 4	12 year-old spayed female mixed breed; Soft tissue sarcoma on the right tarsus	11.2 cm longest diameter 468.8 ml GTV	1225	200	Stable disease	Stable disease
Patient 5	9 year-old male castrated Miniature Pinscher; Soft tissue sarcoma on the right carpus	1.7 cm longest diameter 0.68 mL GTV	11.1	300	Complete response	Complete response
Patient 6	8 year-old male castrated Shih Tzu; Soft tissue sarcoma on the left lateral shoulder	$5 \times 4.2 \times 3.5 \text{ cm}^3$ 135.9 ml GTV	370	300	Progressive disease	Progressive disease

**Table 2.** Treatment prescription characteristics for all canine patients. The injection points are split into groups based on the planned activity per injection.

Dosage/Injections							
Canine patient	Prescribed mean tumor dose (Gy)	Injection points group	Spacing (mm)	Volume (ml)	Number of injections	Activity planned (MBq)/injection	Total activity planned (MBq)
Patient 1	300	#1	4	0.12	31	6.99	435.06
		#2	4	0.15	21	8.73	
		#3	N/A	0.05	12	2.92	
Patient 2	255	#1	5	0.2	75	9.47	710.25
Patient 3	300	#1	5	0.2	18	9.47	170.46
Patient 4	200	#1	6	0.2	70	7	1225
		#2	6	0.3	70	10.5	
Patient 5	300	#1	4	0.06	3	3.33	11.1
		#2	4	0.02	1	1.11	
Patient 6	300	#1	5	0.2	40	9.25	370

administration involved creating activity-specific parallel columns of 20–150  $\mu\text{l}$ , spaced at intervals of 4–6 mm. To achieve the prescribed mean tumor dose, ranging between 200 to 300 Gy, different planned activities were injected (from 11.1 to 1225 MBq). Table 2 shows treatment prescription characteristics, including the planned injection points, for all canine patients.



### 2.3. Stylized phantom-based dosimetry and spatial extension of $^{90}\text{Y}$ -IsoPet™

We performed a retrospective dosimetric evaluation based on the clinical prescription 2D diagrams mentioned above. Using the drawn diagrams and specifications of IsoPet™ injection points, we transferred the points to a grid pattern and placed injections uniformly at the vertices using OpenTOPAS, as shown in figure 1. Each of these injection points represents a column source in OpenTOPAS, resulting in a cylindrically spreading dose distribution for each injection and contributing to the total dose. We then fitted the face of an elliptical cylinder around the points and chose the length to reach the distal end of the contoured gross tumor volume (GTV). The resulting length of this elliptical cylinder was also used to determine the length of each column source. A schematic is provided in figure S1 in the supplementary material. Each injection point was assigned a relative activity value of  $^{90}\text{Y}$ , with some cases featuring multiple injection values. These values were scaled to the true activity by multiplying the simulated activity by a scalar.

To model IsoPet™ seeping into the tumor, we introduced a Gaussian parameter of variable standard deviation represented by sigma. For each tumor, we ran simulations with sigma values ranging from 0 mm up to the half-length between grid points, i.e. 2 mm for a 4 mm grid, at one-half mm intervals. To score the dose in the tumor under the conditions of electronic equilibrium, we created a scorer comprised of a square sheet of voxels fit to the largest half-length of each ellipse and placed it at the midpoint of the cylindrical tumor.

### 2.4. PET/CT scans and Monte Carlo imaging-based dosimetry

PET/CT scans (Celesteion pureVision, Canon Medical, Tustin, CA) were taken immediately after injection at the Small Animal Hospital of the University of Missouri for all canine patients to perform image-based dosimetry. The shape of the field of view was cylindrical, with variable reconstruction diameters based on the patient characteristics, ranging from 240 mm to 550 mm  $\times$  196 mm. For the PET scans, voxel sizes ranged from  $2.04 \times 2.04 \times 2.04 \text{ mm}^3$  to  $4.08 \times 4.08 \times 4.08 \text{ mm}^3$ . The PET signal was reconstructed using the 3D-OSEM method, including attenuation, scattering, normalization, random, detector dead time, and decay corrections (Bryan *et al* 2020). No partial volume corrections were applied. The resulting PET voxel values were quantified in  $\text{Bq ml}^{-1}$ . For the CT, the pixel spacing ranged from  $0.47 \times 0.47 \text{ mm}^2$  to  $1.08 \times 1.08 \text{ mm}^2$  with a slice thickness of 3 mm in all cases.

We employed an adapted version of OpenTOPAS 3.8 to calculate Monte Carlo voxel-based dosimetry (Bertolet *et al* 2021). Using the PET scans, we generated distributed sources in OpenTOPAS to simulate  $^{90}\text{Y}$  emissions according to the radioactive decay data from Geant4 (Hauf *et al* 2013), version 10.7.p3. For each new history, a voxel from the PET was selected with probability proportional to the number of counts in the PET scan. A random origin position was selected within the voxel. We then transported the  $\beta$  particles and subsequent x-rays generated in the  $^{90}\text{Y}$  decays using the standard physics list for electromagnetic processes in

Geant4 (Ivanchenko *et al* 2019). The absorbed dose to water was calculated on the CT grid after  $10^7$  simulated decays using the method proposed by Schneider *et al* (2000) to transform Hounsfield Units into materials for the OpenTOPAS simulation. To determine the statistical uncertainty in our Monte Carlo dose calculation, we calculated the coefficient of variation (CV) in all voxels for each dog.

As a reference to compare with Monte Carlo, we implemented a voxel S-value (VSV) algorithm according to the medical internal radiation dose (MIRD) formalism for analytical voxel-based dosimetry. The rationale for its use in IsoPet<sup>TM</sup> therapy was described elsewhere (Fisher *et al* 2020). For this method, we used our open-source code MIRDCalculator v2.4, available publicly at [github.com/mghro/MIRDCalculator](https://github.com/mghro/MIRDCalculator) and published previously for yttrium-90 radioembolization (Bertolet *et al* 2021). For each patient, we compared both methodologies primarily based on dose-volume histograms (DVHs), by using the anatomical structures of interest delineated by a qualified veterinarian (Fisher *et al* 2020).

### 2.5. Sigma approximation to correlate gel extension with Monte Carlo-based dosimetry

For the stylized phantom-based dosimetry, the DVHs were calculated for the modeled elliptical cylinder representing the GTV. For each canine patient, this resulted in five different DVHs—one for each sigma value representing different spatial spreads of <sup>90</sup>Y-IsoPet<sup>TM</sup>.

To approximate the closest sigma representative of all cases, we performed a dose homogeneity comparison between the stylized phantom and Monte Carlo dosimetry methods. For this purpose, we define the homogeneity index as  $HI = (D_{10\%} - D_{90\%}) / D_p$ , where  $D_{10\%}$  and  $D_{90\%}$  are the minimum doses to 10% and 90% of the target volume, respectively, and  $D_p$  is the prescription (Kataria *et al* 2012). The choice of this metric over values typically used in external beam radiotherapy (e.g.  $D_{5\%}$  and  $D_{95\%}$ ), is based on the linear part of the DVH, excluding the much more pronounced cold and hot spots in internal radiotherapy. Choosing these values provides a more central quantification of the dose distribution, focusing on the core of the tumor rather than its periphery, which was the goal pursued in the injection procedure designed. To avoid bias due to the difference in absolute measured dose between the two methods, we normalized the DVHs to the same mean dose in the target volume. The  $0\Delta HI$  was then calculated for each sigma between the prescription-based dose and the imaging-based dose, allowing a 2nd order spline interpolation over the entire sigma range to determine the theoretical minimum  $\Delta HI$  for each dog.

## 3. Results

### 3.1. Stylized phantom-based dosimetry and sigma variation

Figure 2 illustrates the stylized phantom-based dosimetry for one of the six dogs (patient 2). 2D heat maps show the simulated dose distributions on the axial slices through the tumor volume. The initial injection pattern (as seen in figure 1 for sigma = 0.0 mm) becomes more homogeneous as the gel spreads out from the injection sites (increasing sigma) resulting in a more homogeneous dose distribution. Differential DVHs for each sigma value are shown below their corresponding dose maps. Finally, cumulative DVHs of all simulated doses are shown on the right, indicating a gradual increase in dose homogeneity with increasing sigma, approaching saturation.

### 3.2. Monte Carlo imaging-based dosimetry

Figure 3 summarizes all Monte Carlo simulated results for the imaging-based dosimetry, i.e. dose distributions calculated from the PET-measured activity. CT scans (sagittal/coronal and axial slices) are shown for all six canine patients, with the simulated dose distributions superimposed on the scans. The dose color bars are set from  $D_{90\%}$  to  $D_{2\%}$  of each tumor DVH, with dose values below  $D_{90\%}$  not shown to consistently display the dose mostly within the tumor contour. The cumulative DVHs for all delineated structures are shown on the right, next to the corresponding dose distributions. In addition, the reference DVH calculated based on the MIRD formalism for the tumor is plotted (black dashed line) to compare the Monte Carlo calculation with the analytical reference.

We found agreement between the two methods, with the largest discrepancy observed for patient 5. However, this case involved the smallest tumor volume in the patient cohort (0.68 ml), making direct DVH comparisons more sensitive to differences in tumor size. In addition, we observed tissue density heterogeneities in the tumor volume for this case which may further increase the discrepancies between Monte Carlo calculation and the analytical reference. These heterogeneities are shown in figure S3 in the supplementary material. In addition, the lack of partial volume corrections may have a large impact on image-based uncertainties for small tumor volumes, potentially leading to deviations from the prescribed mean tumor dose in table 1.

Regarding the statistical uncertainty associated with our Monte Carlo simulations, the CV corresponding to the maximum dose ( $D_{max}$ ) in the tumor volume for all patients ranged from 1.5% to 2.3%, except for

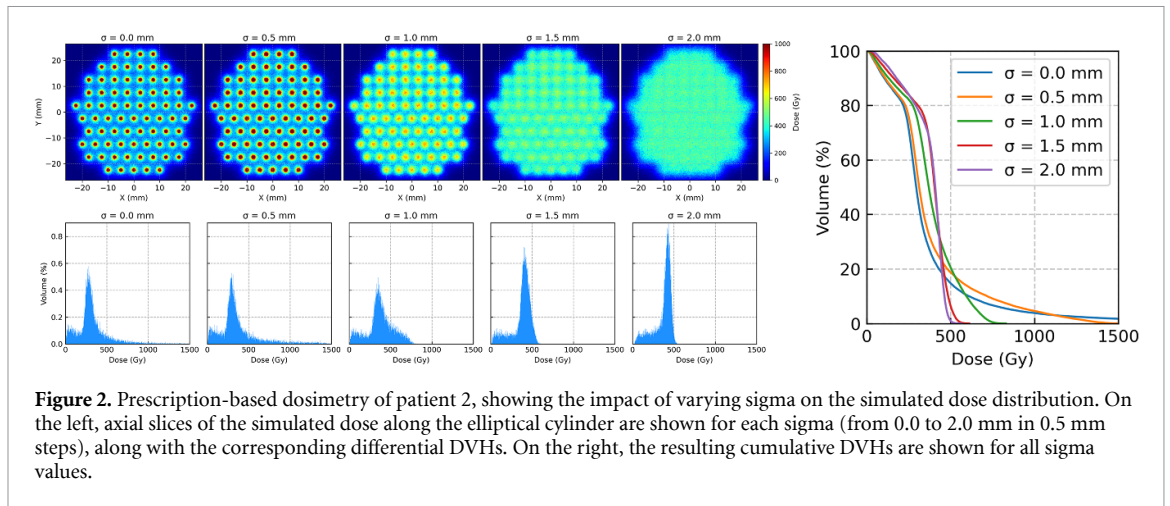


**Figure 2.** Prescription-based dosimetry of patient 2, showing the impact of varying sigma on the simulated dose distribution. On the left, axial slices of the simulated dose along the elliptical cylinder are shown for each sigma (from 0.0 to 2.0 mm in 0.5 mm steps), along with the corresponding differential DVHs. On the right, the resulting cumulative DVHs are shown for all sigma values.

patient 5, whose CV was 10% with an absolute error of 2 Gy. For all other voxels, the CV scales roughly with  $\sqrt{D_{\max}/D}$ , where  $D$  is the dose value to the specific voxel.

### 3.3. Sigma approximation for $^{90}\text{Y}$ -IsoPet™ modeling

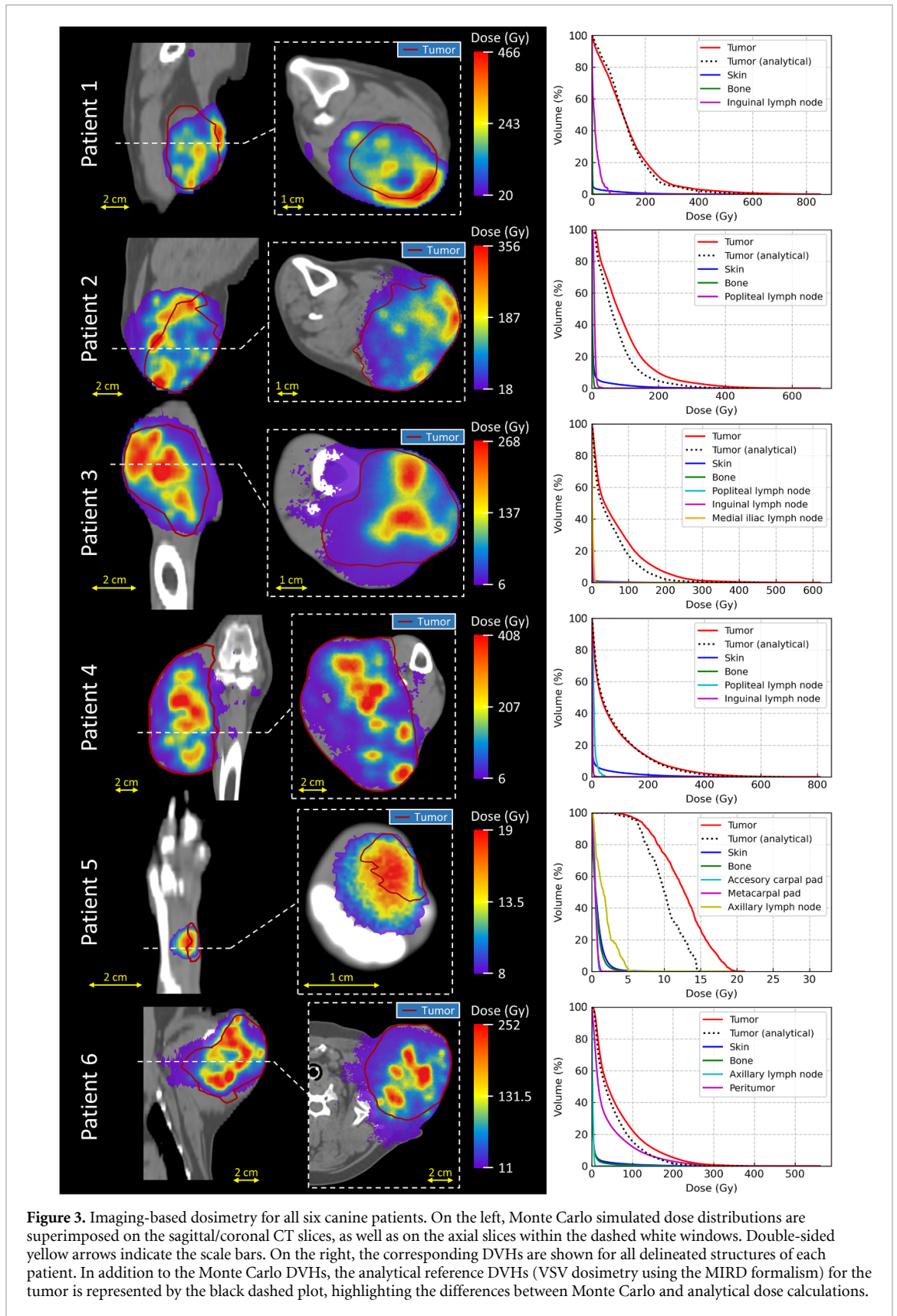
Figure 4 shows the sigma approximation for the spatial spread of  $^{90}\text{Y}$ -IsoPet™. The approximation involved calculating the absolute difference in HI between two dosimetry methods: stylized phantom-based and Monte Carlo imaging-based. For all simulated sigma values, data points representing  $\Delta\text{HI}$  are indicated by square markers. The dashed lines show the 2nd order spline interpolation along the  $x$ -axis (i.e. sigma) used to determine the theoretical minimum  $\Delta\text{HI}$  for each case. The resulting minima are indicated by red triangles. We found that the approximated minimum  $\Delta\text{HI}$  ranged from 0.35 mm to 0.52 mm. Summarizing the six data points into a boxplot (shown at the bottom of the figure) yields a median sigma of approximately 0.44 mm with a standard deviation of 0.05 mm.

## 4. Discussion

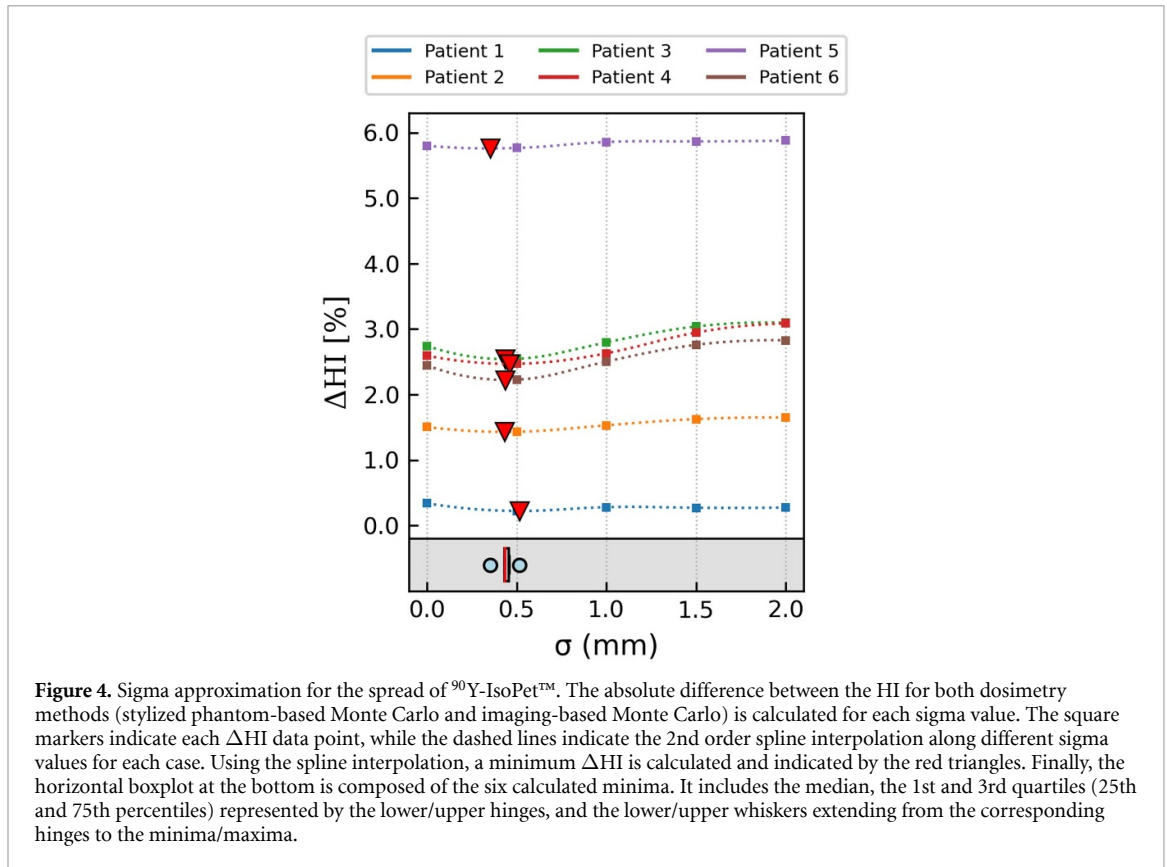
This study adds new insights into the understanding of IsoPet™ therapy, which we expect to be transferable to the RadioGel™ for human patients. This is the second dosimetry study published on IsoPet™. Our approach includes Monte Carlo simulations to provide a more detailed dose calculation, which can be of particular relevance when dealing with soft tissue sarcoma, as tissue density plays a major role in the calculation of dose in radiation therapy (Andreo 2018). Additionally, we studied the dosimetric impact of the spread-out of the gel after its injection and solidification. These simulations offer a new direction to be explored in the dosimetric analysis of this type of therapy.

Dose prescription for IsoPet™ and RadioGel™ therapy is typically reported in terms of mean tumor dose (Fisher *et al* 2020). However, the same mean tumor dose might be achieved through different injection patterns. Analyzing the non-uniformity pattern in the dose distribution is crucial to understanding the radiobiological impact and patient outcome (Pasciak *et al* 2016, 2019). In this study, we analyzed the dose heterogeneity based on the potential spreading of the gel within the tumor based on 2D diagram patterns used in the clinic. Assuming a Gaussian distribution in each injection point, different sigma values lead to specific dose uniformity. We propose to use the homogeneity index (HI) to evaluate the uniformity of the dose distribution in the core of the target volume (Kataria *et al* 2012). The correlation between  $\Delta\text{HI}$  and sigma (figure 4) implies that the gel does not remain static once injected but tends to spread around its injection site and then solidify. This fact provides insights into design-specific injection patterns that might optimize IsoPet™ treatments, potentially leading to better outcomes. Here, the main limitation of our approach is that the initially hand-drawn injection diagrams determine the definition of the elliptical cylinder representing the GTV (as seen in figure 1), while in reality, the outermost injection points may have been slightly outside of the actual GTV.

Dosimetric evaluations to determine  $\Delta\text{HI}$  were performed to compare the planned diagram pattern (2D approach) with the PET image post-injection (3D approach), resulting in considerable uncertainties in extracting firm conclusions. As described in the Materials and Methods section, the PET quantification included different corrections to account for attenuation, scattering, normalization, random errors, detector dead time, and decay, following the methodology described elsewhere (Bryan *et al* 2020). Despite these corrections, the low yield of positron emissions by  $^{90}\text{Y}$  unavoidably translated into poor signal-to-noise



ratios in the PET image, which arguably contributed the most to the overall dose uncertainty. In addition, we expect larger image-based uncertainties in our results for small objects (i.e. patient 5) due to the lack of partial volume corrections. For the 2D approach, we assumed that the volume activity injections were straight rigid cylinders perfused uniformly over the tumor along an arbitrary 2D spatial plane. In reality, needle insertions are generally not perfectly straight, and this deviation from our model may result in



deviations of the actual delivered dose distribution from the simulated one. Furthermore, the choice of an elliptic cylinder to represent the GTV is a first-order approximation impacting the resulting DVHs. Finally, we modeled the spread of the gel according to a Gaussian distribution for each injection point, which may be an oversimplification when dealing with a complex tumor vasculature.

Several potential future studies could be undertaken to improve dosimetric methods in IsoPet and RadioGel<sup>™</sup> therapy. First, treatment planning systems integrated with Monte Carlo calculations will lead to optimizing and personalizing each treatment three-dimensionally, as opposed to the 2D-based prescriptions employed so far. These deviations can be observed by comparing the image-based doses (3D) with the prescribed doses (done over 2D projections). Furthermore, partial volume corrections should be implemented to reduce image-based uncertainties, especially in the case of small tumors.

Imaging-based dosimetry should be the method of choice to prevent large discrepancies between intended and delivered doses. For this one could envision an approach comparable to 3D treatment planning used in brachytherapy (Cunha *et al* 2020). The 3D tumor and injection grid information will be useful to evaluate possible deviations in the injection trajectories and their role in the gel spread effect and dose distribution uniformity. Exploring the effects of radionuclides with different ranges, half-life, and even other emissions in IsoPet and RadioGel<sup>™</sup> could also yield valuable insights, potentially enhancing the efficacy of the treatment. Nonetheless, studying the effect on the response of the spatial non-uniformities in the dose distribution in a larger population is a clear next step, as that would benefit not only this therapy but also other brachytherapy or radiopharmaceutical therapies. This will include investigating specific dosimetric indicators that might correlate with the clinical outcome and use them for treatment planning and optimization. This may be especially relevant when dealing with heterogeneous tumor environments and to explore potential combinations or compensations between different radiation-based modalities.

## 5. Conclusions

We investigated the dosimetry of  $^{90}\text{Y}$ -IsoPet<sup>™</sup> intratumoral therapy in canine patients. Non-uniform absorbed doses were observed despite the spatial spread of the gel after injection, for which we estimate the median spread to be approximately 0.44 mm, resulting in heterogeneous dose distributions within the tumor. These results are consistent with Monte Carlo simulated dose distributions based on PET/CT

imaging. Further studies are needed to incorporate three-dimensional information into dose prescription planning and to study the effect of different physical properties of the radionuclides.

### Data availability statement

All data that support the findings of this study are included within the article (and any supplementary information files).

### Acknowledgments

The authors recognize and appreciate the scientific contributions made by Dr Rebecca Abergel from Berkeley University during the conceptualization and execution of this article. We would also like to thank the Clinical Research Office and the Comparative Oncology, Radiobiology, and Epigenetics Laboratory at the University of Missouri Veterinary Health Center for their contributions to the veterinary clinical trial.

### Funding

This work was funded by the NIH/NCI Award No. R00CA267560: ‘Radiation dosimetry for  $\alpha$ -particle radiopharmaceutical therapy and application to pediatric neuroblastoma’, and the NIH/NCI Grant No. R01CA187003: ‘TOPAS-nBio, a Monte Carlo tool for radiation biology research’. Funding for the canine study and all IsoPet™ materials was provided by Vivos, Inc.

### ORCID iDs

Mislav Bobić  <https://orcid.org/0000-0002-9409-8680>  
Carlos Huesa-Berral  <https://orcid.org/0000-0003-2290-0176>  
Louis Kunz  <https://orcid.org/0009-0008-6526-6025>  
Jan Schuemann  <https://orcid.org/0000-0002-7554-8818>  
Charles A Maitz  <https://orcid.org/0000-0003-2075-3926>  
Alejandro Bertolet  <https://orcid.org/0000-0002-9890-693X>

### References

- Andreo P 2018 Monte Carlo simulations in radiotherapy dosimetry *Radiat. Oncol.* **13** 121
- Bentzen S M, Constine L S, Deasy J O, Eisbruch A, Jackson A, Marks L B, Ten Haken R K and Yorke E D 2010 Quantitative analyses of normal tissue effects in the clinic (QUANTEC): an introduction to the scientific issues *Int. J. Radiat. Oncol. Biol. Phys.* **76** S3–9
- Bertolet A, Wehrenberg-Klee E, Bobić M, Grassberger C, Perl J, Paganetti H and Schuemann J 2021 Pre- and post-treatment image-based dosimetry in 90Y-microsphere radioembolization using the TOPAS Monte Carlo toolkit *Phys. Med. Biol.* **66** 244002–2
- Bray J P 2016 Soft tissue sarcoma in the dog—part 1: a current review *J. Small Animal Pract.* **57** 510–9
- Bryan J, Lunceford J and Bai B 2020 Evaluation of PET image quality using non-conventional isotopes *J. Nucl. Med.* **61** 1516–6 (available at: [https://jnm.snmjournals.org/content/61/supplement\\_1/1516](https://jnm.snmjournals.org/content/61/supplement_1/1516))
- Cantley J L, Fisher D R, Lin S, Albani D M, Zorrilla A and Bolch W E 2017 Radiation dose to non targeted tissues of the eye during polymer-based delivery of 90Y to ocular melanoma of the choroid *Biomed. Phys. Eng. Express* **3** 035024
- Chansanti O, Jahangiri Y, Matsui Y, Adachi A, Geeratikun Y, Kaufman J A, Kolbeck K J, Stevens J S and Farsad K 2017 Tumor dose response in Yttrium-90 resin microsphere embolization for neuroendocrine liver metastases: a tumor-specific analysis with dose estimation using SPECT-CT *J. Vascular Intervent. Radiol.* **28** 1528–35
- Cunha J A M, Flynn R, Bélanger C, Callaghan C, Kim Y, Jia X, Chen Z and Beaulieu L 2020 Brachytherapy future directions *Semin. Radiat. Oncol.* **30** 94–106
- DeLaney T F, Trofimov A V, Engelsman M and Suit H D 2005 Advanced-technology radiation therapy in the management of bone and soft tissue sarcomas *Cancer Control* **12** 27–35
- Dennis M M, McSparran K D, Bacon N J, Schulman F Y, Foster R A and Powers B E 2010 Prognostic factors for cutaneous and subcutaneous soft tissue sarcomas in dogs *Vet. Pathol.* **48** 73–84
- Fisher D R 2021 Radiation safety for Yttrium-90-polymer composites (IsoPet™) in therapy of solid tumors *Health Phys.* **120** 510–6
- Fisher D R, Fidel J and Maitz C A 2020 Direct interstitial treatment of solid tumors using an injectable Yttrium-90-polymer composite *Cancer Biother. Radiopharm.* **35** 1–9
- Fisher D, Fidel J and Duffy M 2018 Interstitial therapy of feline sarcoma using an injectable Y-90 polymer composite (IsoPet) *J. Nucl. Med.* **59** 1257–7 (available at: [https://jnm.snmjournals.org/content/59/supplement\\_1/1257](https://jnm.snmjournals.org/content/59/supplement_1/1257))
- Garin E et al 2020 Personalised versus standard dosimetry approach of selective internal radiation therapy in patients with locally advanced hepatocellular carcinoma (DOSISPHERE-01): a randomised, multicentre, open-label phase 2 trial *Lancet Gastroenterol. Hepatol.* **6** 17–29
- Hauf S, Kuster M, Batič M, Dalla Betta G F, Hoffmann H, Lang P, Neff S, Pia M G, Weidenspointner G and Zoglauer A 2013 Radioactive decays in Geant4 *IEEE Trans. Nucl. Sci.* **60** 2966–83
- Hoefkens F, Dehandschutter C, Somville J, Meijnders P and Van Gestel D 2016 Soft tissue sarcoma of the extremities: pending questions on surgery and radiotherapy *Radiat. Oncol.* **11** 136

- Ivanchenko V *et al* 2019 Progress of Geant4 electromagnetic physics developments and applications *EPJ Web Conf.* **214** 02046–6
- Kataria T, Sharma K, Subramani V, Karrthick K P and Bisht S S 2012 Homogeneity index: an objective tool for assessment of conformal radiation treatments *J. Med. Phys.* **37** 207–13
- Miller E D, Xu-Welliver M and Haglund K E 2014 The role of modern radiation therapy in the management of extremity sarcomas *J. Surg. Oncol.* **111** 599–603
- Pasciak A S *et al* 2019 The number of microspheres in Y90 radioembolization directly affects normal tissue radiation exposure *Eur. J. Nucl. Med. Mol. Imaging* **47** 816–27
- Pasciak A S, Bourgeois A C and Bradley Y C 2016 A microdosimetric analysis of absorbed dose to tumor as a function of number of microspheres per unit volume in 90Y radioembolization *J. Nucl. Med.* **57** 1020–6
- Schneider W, Bortfeld T and Schlegel W 2000 Correlation between CT numbers and tissue parameters needed for Monte Carlo simulations of clinical dose distributions *Phys. Med. Biol.* **45** 459–78
- Withrow S P 2007 *Small Animal Clinical Oncology* (Saunders Elsevier)